Scripta Materialia 158 (2019) 116–120

Contents lists available at ScienceDirect

Scripta Materialia

journal homepage: www.elsevier.com/locate/scriptamat

Fatigue behavior of ultrafine grained triplex $Al_{0.3}CoCrFeNi$ high entropy alloy

Kaimiao Liu [a], Mageshwari Komarasamy [a], Bharat Gwalani [b], Shivakant Shukla [a], Rajiv S. Mishra [a,b,*]

[a] Center for Friction Stir Processing, Department of Materials Science and Engineering, University of North Texas, Denton, TX 76207, USA
[b] Advanced Materials and Manufacturing Processes Institute, University of North Texas, Denton, TX 76207, USA

ARTICLE INFO

Article history:
Received 30 July 2018
Received in revised form 26 August 2018
Accepted 27 August 2018
Available online xxxx

Keywords:
High entropy alloy
Ultrafine grained
Tensile
Fatigue
Deformation twins

ABSTRACT

Ultrafine grained (UFG) alloys suffer from limited strain hardening hence reduced ductility. Incorporation of deformation twinning can overcome this limitation. An $Al_{0.3}CoCrFeNi$ high-entropy alloy was thermo-mechanically processed to yield a UFG triplex microstructure (d_{avg}: 0.71 ± 0.35 μm) with FCC, and hard B2 and sigma phases. The annealed material exhibited an exceptional strength-ductility combination with ultimate tensile strength (UTS) of ~1.1 GPa and elongation of ~25%. Furthermore, the alloy showed excellent fatigue resistance with an endurance limit of ~0.43 UTS. Remarkable mechanical properties are attributed to the formation of extensive deformation nanotwins and increased dislocation accumulation capability.

Introduction

A new class of alloy system known as high entropy alloys (HEAs) or complex concentrated alloys (CCAs) was developed independently by Yeh et al. [1] and Cantor et al. [2]. HEA was conceptualized based on maximizing the configurational entropy of the alloy system by mixing equiatomic or non-equiatomic quantities of five or more elements to form a complete solid solution. However, the recent definition has evolved to include ternary compositions as well as compositions that form intermetallic compounds; hence the current designation CCAs [3]. Large negative enthalpy of mixing overcomes the effect of the entropy of mixing contribution to Gibbs free energy, thereby leading to the formation of second phases. Considering both configurational entropy and enthalpy of mixing, HEAs have a potential for solid solution strengthening and precipitation hardening, which contributes to high strength. For example, with increasing Al content, $Al_xCoCrFeNi$ system transforms from single-phase face-centered cubic (FCC) structure to FCC+B2 (NiAl), then to body-centered cubic (BCC/B2)+FCC, and finally to single-phase BCC. B2 phase is known to increase FCC matrix strength [4]. In general, FCC HEAs exhibit low stacking fault energy (SFE) [5]. It leads to the easy formation of stacking faults, deformation twins, and subsequent interaction of dislocations with these faults generally resulting in excellent work hardenability, hence good ductility [6]. The majority of investigations have focused on the tensile and compressive deformation behaviors of HEAs [4], only four reports have been published on the fatigue behavior of HEAs. Hemphill et al. [7] examined the fatigue behavior of cold-rolled $Al_{0.5}CoCrCuFeNi$, where the fatigue failure initiated from the Al_2O_3 inclusions and pre-existing microcracks. With the same composition as Hemphill et al. [7], Tang et al. [8] investigated the effect of raw material purity on fatigue behavior. Alloys made with high purity elements exhibited better properties; nevertheless, fatigue crack initiated at the shrinkage pores. Furthermore, dense deformation nano-twins were observed near the crack initiation site. Pre-notched as-cast $Al_{0.2}CrFeNiTi_{0.2}$ and $AlCrFeNi_2Cu$ tested using three-point bending showed that two-phase HEAs exhibited lower toughness than single-phase HEAs [9]. Recently, Shukla et al. [10] observed that crack initiation was delayed due to B2 (BCC) precipitates blocking the path of persistent slip bands in a heat treated eutectic $AlCoCrFeNi_{2.1}$ HEA. A detailed investigation of microstructural evolution during fatigue and subsequent fatigue damage evolution is still lacking in any HEAs.

The current study elucidates deformation mechanisms in an ultrafine-grained (UFG) $Al_{0.3}CoCrFeNi$ HEA under fully reversible bending fatigue loading. Initial and post-fatigue microstructural analyses were carried out using scanning electron microscopy (SEM), orientation imaging microscopy (OIM) and transmission electron microscopy (TEM) to elucidate the significance of various microstructural elements on the fatigue deformation mechanisms.

Experimental

The alloy was prepared using vacuum arc melting, and five flips were done to homogenize the melt chemical composition. The cast

* Corresponding author.
E-mail address: Rajiv.Mishra@unt.edu (R.S. Mishra).

https://doi.org/10.1016/j.scriptamat.2018.08.048
1359-6462/

samples were solutionized at 1200 °C for 48 h in vacuum with subsequent furnace cooling. The rectangular piece was then subjected to ~84% cold rolling reduction to achieve a final thickness of ~1.5 mm. The rolled material was subsequently annealed at 700 °C for 36 h to attain a completely recrystallized UFG microstructure. Sub-sized tensile and fatigue samples were milled with a computer numerical control machine. Tensile samples with gage length ~5 mm, width ~1.2 mm, and thickness ~1.1 mm were tested using a computer-controlled mini-tensile machine at an initial strain rate of 10^{-3} s^{-1}. Fully reversed ($R = -1$) bending fatigue tests were performed with a custom-made tabletop fatigue testing machine at 20 Hz. Sample dimensions and machine details are given in [11]. Tensile and fatigue samples were polished with SiC papers to 1200 grit, and final polishing with 1 μm diamond suspension. Fatigue and microscopy samples were further polished with 0.05 and 0.02 μm colloidal silica suspensions. Back-scattered electron microscopy (BSE) was carried out on the FEI Nova NanoSEM230. Grain size and distribution, phase fraction of FCC, B2, and sigma (σ) fraction were obtained using OIM on FEI Nova NanoSEM230, with a 20 kV accelerating voltage and 6.1 nA current. X-ray diffraction (XRD) was used to further confirm the presence of three phases using Rigaku Ultima III high-resolution XRD with Cu Kα radiation. TEM analysis was conducted on both before and after fatigue tested samples using FEI Tecnai G2 TF20™ at 200 kV and samples were prepared using focused ion beam (FIB) (FEI Nova 200 NanoLab).

Results and discussion

Initial microstructural analysis at various locations after 700 °C for 36 h annealing treatment is presented in Fig. 1. The BSED image in Fig. 1(a) shows several dark-contrast precipitates of different morphologies. These precipitates are eventually characterized as ordered BCC (B2) and σ phases formed in an FCC matrix (bright contrast, in BSED image). High magnification image of fine B2 and σ is displayed in the inset of Fig. 1(a). Finer B2 and σ precipitates formed simultaneously at the grain interior and boundaries during annealing heat treatment. Fig. 1(b) shows an inverse pole figure (IPF) map where a random crystallographic orientation was observed after cold rolling and annealing. FCC matrix exhibited an average grain size of 0.71 ± 0.35 μm, which is in the ultra-fine grained (UFG) regime. UFG materials in general display extraordinary tensile strength, but inadequate ductility due to its inability to store dislocations [12]. OIM phase fraction analysis obtained from the same region provided FCC, B2, and σ fraction as 81%, 14%, and 5%, respectively (Fig. 1(c)). XRD was done to confirm the presence of these phases, Fig. 1(d). Annealing treatment (700 °C for 36 h) facilitated the formation of tetragonal Fe-Cr-rich σ phase, which is usually observed in Fe-Cr-containing alloys in the temperature range of 500 °C–750 °C [10]. In addition to micron-sized B2 in BSE-SEM analysis, nano-sized B2 and σ precipitates were also observed. The bright-field (BF) TEM in Fig. 1(e) shows FCC, σ and B2 phases. Big particle on the top left of the BFTEM image was indexed as σ phase, as confirmed by the diffraction pattern from [001] zone axis (ZA), (Fig. 1(e_1)). The [001] micro-diffraction pattern established that the matrix was FCC phase (Fig. 1(e_2)). The micro-diffraction pattern of oval-shaped precipitate on the grain boundary was consistently indexed as a B2 (ordered BCC) crystal structure (Fig. 1(e_3)). The STEM EDX revealed the composition of different phases (Fig. 1(f_{1-2})). A compositional profile confirmed σ phase had 78% Cr, and 17.5% Fe whereas the B2 phase had 29% Al and 50% Ni (all compositions are in at.%). All the microstructural features mentioned above — for example, B2, σ, and ultrafine grains — will have effects on fatigue deformation evolution and subsequent failure.

Both engineering and true stress-strain curves are shown in Fig. 2(a). $Al_{0.3}$CoCrFeNi HEA exhibited extraordinary yield strength (YS) of

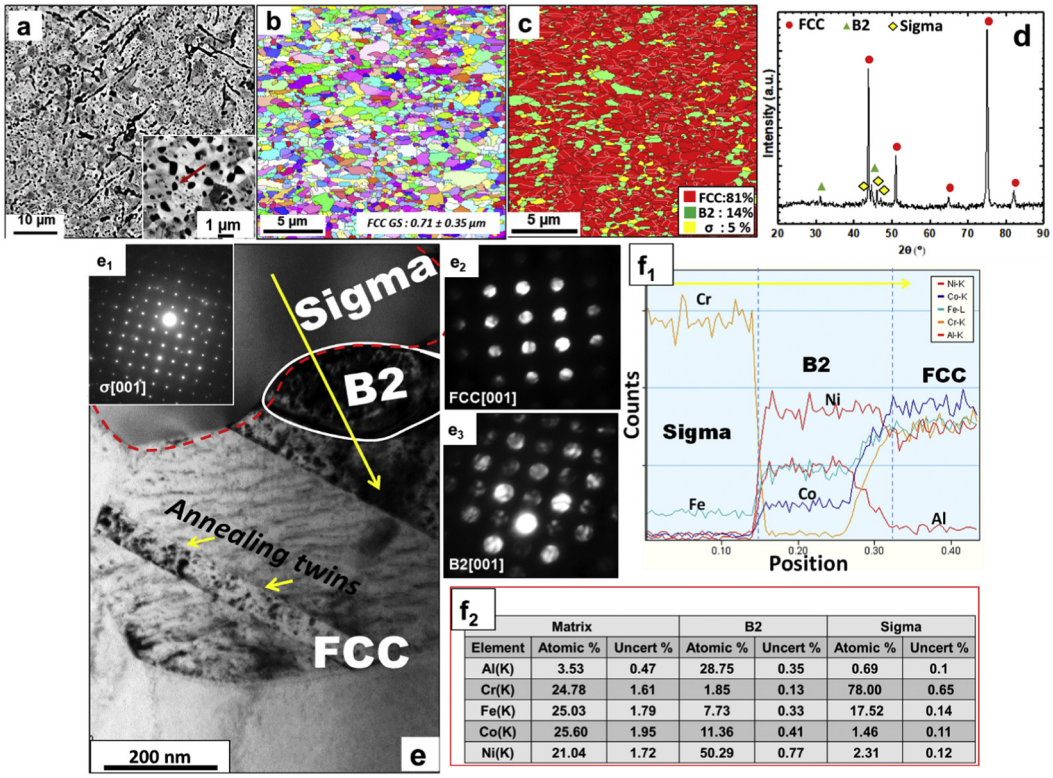

	Matrix		B2		Sigma	
Element	Atomic %	Uncert %	Atomic %	Uncert %	Atomic %	Uncert %
Al(K)	3.53	0.47	28.75	0.35	0.69	0.1
Cr(K)	24.78	1.61	1.85	0.13	78.00	0.65
Fe(K)	25.03	1.79	7.73	0.33	17.52	0.14
Co(K)	25.60	1.95	11.36	0.41	1.46	0.11
Ni(K)	21.04	1.72	50.29	0.77	2.31	0.12

Fig. 1. *Initial microstructural analysis.* a) BSE image showing FCC matrix with coarse and fine-scale second-phase precipitates. High magnification SEM image in the inset shows the smaller precipitates pointed by the red arrow, (b) IPF map with high angle boundaries depicted by black lines, (c) EBSD phase map of the same region as (b) highlighting FCC (red), B2 (green), and σ (yellow) phases with white color-coded CSL boundaries and black color-coded grain boundaries, (d) XRD results show the presence of three phases, (e) the BFTEM shows FCC, σ, and B2 phases, and the presence of annealing twins, (e_{1-3}) [001] micro-diffraction patterns of σ, FCC, and B2 phase, respectively, (f_{1-2}) STEM-EDX compositional-profile showing the change in composition, and spot EDX compositions obtained from the three phases. (For interpretation of the references to color in this figure legend, the reader is referred to the web version of this article.)